Cancer Cell
Article

Enhanced Paracrine FGF10 Expression Promotes Formation of Multifocal Prostate Adenocarcinoma and an Increase in Epithelial Androgen Receptor

Sanaz Memarzadeh,[1] Li Xin,[2] David J. Mulholland,[3] Alka Mansukhani,[6] Hong Wu,[3] Michael A. Teitell,[4] and Owen N. Witte[2,3,5,*]
[1]Department of Obstetrics and Gynecology
[2]Departments of Microbiology, Immunology, and Molecular Genetics
[3]Departments of Molecular and Medical Pharmacology
[4]Departments of Pathology and Laboratory Medicine
David Geffen School of Medicine
[5]Howard Hughes Medical Institute
University of California, Los Angeles, Los Angeles, CA 90095, USA
[6]Department of Microbiology, New York University School of Medicine, New York, NY 10016, USA
*Correspondence: owenw@microbio.ucla.edu
DOI 10.1016/j.ccr.2007.11.002

SUMMARY

Enhanced mesenchymal expression of FGF10 led to the formation of multifocal PIN or prostate cancer. Inhibition of epithelial FGFR1 signaling using DN FGFR1 led to reversal of the cancer phenotype. A subset of the FGF10-induced carcinoma was serially transplantable. Paracrine FGF10 led to an increase in epithelial androgen receptor and synergized with cell-autonomous activated AKT. Our observations indicate that stromal FGF10 expression may facilitate the multifocal histology observed in prostate adenocarcinoma and suggest the FGF10/FGFR1 axis as a potential therapeutic target in treating hormone-sensitive or refractory prostate cancer. We also show that transient exposure to a paracrine growth factor may be sufficient for the initiation of oncogenic transformation.

INTRODUCTION

The multifocal nature of human prostate cancer is elusive, and mechanisms accounting for this histologic presentation are poorly understood. It is not uncommon to identify areas of cancer adjacent to PIN and even normal prostate tubules in human prostatectomy specimens. This degree of heterogeneity has resulted in the Gleason scoring system, which grades the histologic severity of representative sections as a prognostic indicator of clinical behavior (Bostwick and Foster, 1999).

Heterogeneous genetic instability in the glandular epithelium due to telomerase shortening or infection with viruses such as BK, JC, and a recently described retroviral isolate are two mechanisms by which multifocal disease can occur (Das et al., 2004; Dong et al., 2007; Vukovic et al., 2003; Zambrano et al., 2002). Another widely proposed theory that may explain this multifocal heterogeneity is "field effect," implicating global changes in the prostate that can subsequently give rise to independent polyclonal foci of disease (Harding and Theodorescu, 2000). Perturbations in the stroma may provide a mechanism by which a global cancer-initiating microenvironment can be instigated (Harding and Theodorescu, 2000).

Interactions between stroma and epithelium are critical for development, and alterations in this homeostatic

SIGNIFICANCE

Mechanisms underlying the multifocal nature of human prostate cancer are poorly understood. Using an in vivo reconstitution system that relies on epithelial-stromal interactions, we show that enhanced expression of mesenchymal FGF10, an essential gene for prostate development, led to the formation of well-differentiated, multifocal prostate adenocarcinoma. Paracrine FGF10 signaling caused intrinsic changes in adjacent adult wild-type epithelium, demonstrated by an increase in epithelial androgen receptor (AR) expression, and the development of hormone-refractory disease. FGF10-induced prostatic intraepithelial neoplasia (PIN) or adenocarcinoma could persist in an FGF10-low microenvironment, likely as a result of sustained epithelial changes that evade chronic dependence on this growth factor. We demonstrate a mechanism for the formation of multifocal prostate cancer.

balance can lead to neoplastic transformation (Kalluri and Zeisberg, 2006). Stromal cells are key regulators of adjacent epithelium in multiple epithelial tumor models such as mammary gland (Cheng et al., 2005), skin (Seftor et al., 2005), prostate (Bhowmick et al., 2004a; Hill et al., 2005), and stomach cancers (Bhowmick et al., 2004a). In the normal setting and in these cancer models, epithelial control is exerted by paracrine influences of the adjacent stroma. Paracrine factors stimulate growth and expand the adjacent epithelia by interacting with transforming growth factor β (TGF-β), fibroblast growth factor (FGF), epidermal growth factor (EGF), and insulin-like growth factor (IGF) family receptors (Bhowmick et al., 2004b).

The FGF receptor (FGFR) signaling cascade exemplifies the importance of epithelial and mesenchymal paracrine crosstalk through a diverse set of ligands and receptors that are compartmentalized in the stroma or epithelium (Powers et al., 2000). FGF10 is predominantly expressed in the mesenchyme of the developing prostate gland and is an essential gene for prostate development (Donjacour et al., 2003). In vitro data suggest that FGF10 has mitogenic actions on prostate epithelium and not stroma (Thomson and Cunha, 1999). FGF10 binds preferentially to the IIIb isoform of FGFR1 and FGFR2 (Kwabi-Addo et al., 2004; Lu et al., 1999). Both of these receptors are expressed in the normal prostate epithelium (Kwabi-Addo et al., 2004; Lin et al., 2007; Lu et al., 1999).

Several lines of evidence indicate that altered expression of the FGF/FGFR signaling axis may be important in prostate pathology. *FGF10* transcripts have been detected in stroma derived from benign human prostatic hyperplasia specimens (Nakano et al., 1999). A thorough analysis of FGF10 expression is lacking in human prostate cancer. In the Dunning rat tumor model, FGF10 expression has been detected in the stroma and not epithelium of well-differentiated tumors (Lu et al., 1999). Increased expression of FGFR1 is seen in both human prostate cancer and animal models, such as TRAMP tumors with progression to poorly differentiated adenocarcinoma (Huss et al., 2003; Sahadevan et al., 2007). The role of FGFR2 in prostate cancer is dependent on the expression of its specific isoform (Kwabi-Addo et al., 2004). Activation of the FGFR2 IIIb isoform, the binding partner for FGF10, is thought to have a role in maintaining prostatic epithelial homeostasis, and overexpression of this receptor in neoplastic cells can restore differentiation (Feng et al., 1997; Matsubara et al., 1998).

Previous studies have investigated the role of FGFR1 and FGFR2 in the progression of prostate cancer (Freeman et al., 2003). In a transgenic mouse model, activation of FGFR1 led to formation of PIN, while activation of FGFR2 caused no discernable phenotype (Freeman et al., 2003). Autocrine epithelial overexpression of FGF7, also a stromal gene and a homolog of *FGF10*, in a transgenic animal model led to the formation of prostate hyperplasia after 1 year (Foster et al., 2002). These models used epithelial-based FGF expression and did not promote FGF signaling from the mesenchyme. As such, they do not examine the role of mesenchymal FGF on adjacent epithelial biology.

We set out to test whether enhanced expression of mesenchymal FGF10 would be sufficient to drive transformation of adult prostate epithelium. We hypothesized that the mitogenic paracrine effects of FGF10 could be regional and predominantly on the neighboring epithelial cells. To investigate the potential biologic effects of FGF10-mediated signaling in the development of prostate cancer, we used a tissue recombination prostate regeneration system (Cunha and Lung, 1978), further modified into a dissociated single-cell reconstitution method (Xin et al., 2003). In this model, adult dissociated prostate epithelial cells are combined with embryonic urogenital sinus mesenchyme (UGSM) and grafted under the kidney capsule of a SCID mouse, resulting in formation of prostate gland-like structures (Xin et al., 2003). This model allows for genetic manipulation of both compartments of the prostate gland, the epithelium and the mesenchyme, independently and, in contrast to previously published transgenic animal models, enables us to study the effects of paracrine factors on adult prostate epithelial cells.

We show that enhanced expression of mesenchymal FGF10 was sufficient for the formation of well-differentiated prostate carcinoma. The disease pattern observed was multifocal and similar to human prostate cancer when the number of FGF10-expressing UGSM cells was diluted. Inhibition of FGFR1 signaling with dominant-negative (DN) FGFR1 could reverse the neoplastic phenotype even in the presence of excess mesenchymal FGF10. Paracrine FGF10 led to an increase in epithelial androgen receptor, and upon castration, FGF10 induced androgen-independent survival and proliferation. FGF10-induced PIN or adenocarcinoma persisted in an FGF10-low microenvironment, with sustained activation of the AR machinery. Paracrine FGF10 synergized with cell-autonomous activated AKT and resulted in the formation of poorly differentiated adenocarcinoma.

RESULTS

Paracrine Signaling Mediated by Mesenchymal FGF10 Is Sufficient for the Histologic Transformation of the Adjacent Prostate Epithelium

Retroviral constructs were designed to express GFP or FGF10 and GFP (Figure S1A in the Supplemental Data available with this article online). UGSM was infected with either control vector (GFP) or FGF10-GFP retrovirus. Expression of secreted FGF10 was confirmed by western blot (Figure S1B). FACS analysis confirmed greater than 90% infection of the UGSM cells (Figure S1C).

Dissociated adult murine prostate cells (1×10^5) were combined with UGSM cells (1×10^5) infected either with control or FGF10-expressing vectors and engrafted under the kidney capsule of CB.17 $^{SCID/SCID}$ mice (Xin et al., 2003). After 8 weeks, mice were sacrificed, and grafts were dissected off the kidney (Figure 1A). The FGF10-expressing grafts weighed greater than twice the control grafts (Figure 1A).

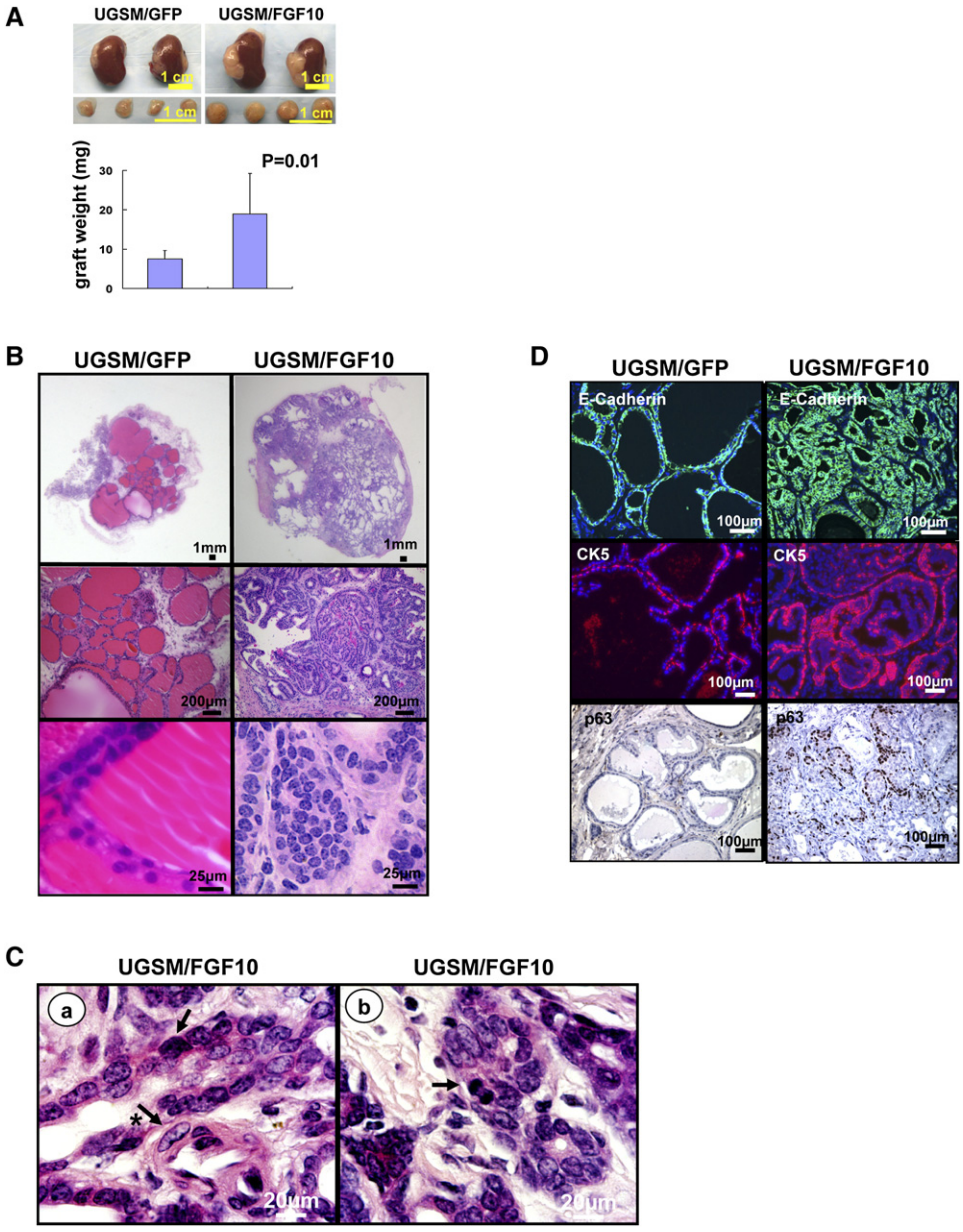

Figure 1. Paracrine FGF10 Expression Led to Well-Differentiated Adenocarcinoma and an Expansion of Both Luminal and Basal Cells

(A) Transilluminating image and weight (mean ± SD) of regenerated tissue from wild-type epithelia (1×10^5) combined with GFP- or FGF10-expressing mesenchyme (1×10^5) placed in the regeneration system.

(B) H&E analysis of FGF10 UGSM- and GFP UGSM-regenerated tissue.

(C) High-power (1000×) magnification of FGF10-induced adenocarcinoma demonstrating atypical (arrow) or large nuclei (arrow and asterisk) in (Ca) and evidence of mitotic figures (arrow) in (Cb).

(D) Immunohistochemical analysis of the regenerated tissue using antibodies against E-cadherin, CK5, and P63.

Histologic analysis of the control grafts revealed epithelial glands two layers thick with abundant luminal secretions (Figure 1B). In contrast, FGF10 grafts showed an increased number of small glandular structures, one cell layer thick, containing cells with increased nuclear to cytoplasmic ratios, prominent multiple nucleoli, scattered apoptotic bodies, and occasional mitotic figures (Figures 1B and 1C). These features were diagnostic of well-differentiated prostate adenocarcinoma in 10/10 independent paracrine FGF10-regenerated grafts (Figures 1B and 1C) (Shappell et al., 2004). The commercially available antibodies for FGF10 can not detect this protein by immunohistochemistry. Therefore, GFP faithfully expressed by an internal ribosomal entry site (IRES) in the FGF10-expressing constructs was localized in the mesenchymal compartment of regenerated grafts (Figure S1D). Expression

of GFP provided an indirect marker for overexpression of mesenchymal FGF10 (Figure S1D). The contour of the epithelial cells was outlined by pancytokeratin staining (Figure S1D). Enhanced expression of FGF10 was confirmed with western blot analysis in three independent FGF10-regenerated grafts (Figure S1E).

To characterize the expanded epithelial cell population, immunohistochemistry was performed for the epithelial markers cytokeratin 5 (CK5), CK8, p63, and E-cadherin (Figure 1D and Figure S2). Glands from FGF10 grafts expressed E-cadherin (Figure 1D, top panel) and cytokeratin 8 (Figure S2A) confirming the epithelial nature of these cells. We detected an approximately 3-fold expansion of p63-positive cells in FGF10-expressing grafts (Figure 1D, bottom panel). We also observed a dramatic expansion of the luminal cells in FGF10 grafts compared to control (Figure S2A). Paracrine FGF10 signaling resulted in the formation of a glandular adenocarcinoma in a background of prostatic hyperplasia. Previous models for prostate cancer led to the formation of luminal or neuron-endocrine carcinoma (Freeman et al., 2003; Greenberg et al., 1995; Majumder et al., 2003; Wang et al., 2003). In our model we observed an expansion of luminal cells expressing CK8 (Figure S2A) in addition to an expansion of basal cells expressing CK5/P63 (Figure S2B and Figure 1D, bottom two panels).

Paracrine FGF10 Promotes Localized Transformation in the Prostate Regeneration System

We asked whether the transforming effects of FGF10 were local or extended beyond the source of FGF10-secreting cells. We placed one graft with FGF10-secreting UGSM adjacent to a second graft with normal UGSM cells (Figure 2A). We then set up a dilution series of FGF10-secreting cells such that the number of FGF10-secreting UGSM was decreased in a logarithmic fashion by substituting normal UGSM (Figure 2C). To measure the proliferation of regenerating epithelium at 6 weeks, mice were injected with bromodeoxyuridine (Brdu) i.p. (80 mg/kg) and sacrificed after 2 hr. Grafts were harvested and stained with Brdu antibody (Figure 2B and Figure S3). The Brdu-labeled epithelia were counted and averaged in four independent high-power fields on each end of the two adjacent grafts as well as the middle portion.

Two obviously distinct histologic zones were identified when an FGF10-secreting graft was placed adjacent to a normal graft (Figure 2B). One end of the graft with normal UGSM showed normal prostatic tubules, while the opposite end with FGF10-secreting mesenchyme revealed well-differentiated adenocarcinoma (Figure 2B). FGF10 led to a local increase in the number of proliferating epithelial cells, as shown by increased epithelial Brdu uptake in the FGF10-containing region (Figure S3). The amount of Brdu uptake was 5-fold less on the control side compared to the cancer side of the graft, suggesting that the effects of FGF10 were localized (Figure S3).

Decreasing the number of FGF10-secreting UGSM led to a less severe phenotype, suggesting that the transforming effects of paracrine FGF10 are dose dependent (Figure 2C). In the presence of 50% FGF10 UGSM adenocarcinoma was noted, whereas progression to PIN adjacent to possibly microinvasive carcinoma (1:10) and PIN (1:100) were observed in FGF10-diluted grafts, culminating in normal prostatic epithelium when the FGF10-secreting mesenchymal cells were diluted by a factor of 1000. Microinvasive adenocarcinoma and hyperplastic tubules appeared adjacent to PIN lesions and normal prostate glands in 1:10 and 1:100 diluted samples. This disease pattern resembled the heterogeneous histologic appearance of human prostate cancer and PIN (Figure 2C). To examine the location of FGF10-secreting UGSM cells, the expression of GFP was examined as an indirect marker for FGF10, in the diluted 1:10 and 1:100 specimens (Figures 2Da–2Dl). We observed the presence of GFP-positive, hence FGF10-secreting, UGSM cells adjacent to areas of microinvasive carcinoma and PIN lesions (Figures 2Dc, 2Dd, 2Di, and 2Dj). The expression of GFP was noted to be absent adjacent to normal regenerated tubules (Figures 2De, 2Df, 2Dk, and 2Dl).

Our data indicate that regional PIN and multifocal adenocarcinoma could be recapitulated by altered adjacent cancer stromal cells, similar to the paracrine effects of FGF10-overexpressing mesenchyme.

Inhibition of FGFR1 Signaling by DN FGFR1 Reverts FGF10-Induced Adenocarcinoma

We hypothesized that blocking FGFR1 and/or FGFR2 signaling would lead to formation of normal tubules even in the presence of excess mesenchymal FGF10. To test our hypothesis, lentiviral vectors were constructed to express DN FGFR1 and DN FGFR2, flag tagged for better detection on western blot (Figure 3A) (Li et al., 1994). The *DN FGFR1* and *DN FGFR2* constructs encode proteins that are truncated downstream of the transmembrane domain and are signaling defective (Li et al., 1994). The lentiviral constructs express the red fluorescent protein (RFP) to mark the site of expression of the DN FGFR. Dissociated prostate epithelial cells were infected with either vector control, DN FGFR1, or DN FGFR2 and combined with equal numbers of FGF10 and WT UGSM and grafted for 6–8 weeks.

Expression of either DN construct resulted in formation of smaller grafts compared to vector control (Figure 3B). Fluorescence microscopy of the regenerated grafts was performed. The frequency of red tubules composed of DN FGFR1 or DN FGFR2 was significantly lower compared to vector control. Multiple sections of regenerated tissue were reviewed to identify relatively rare red tubules in the grafts containing DN FGFR1 or DN FGFR2. The decrease in the size and the rarity of red tubules in the DN-regenerated tissue can be explained by the variation in the copy number and integration frequency of lentiviral DN constructs in the regenerating epithelia. High doses of either of the DN constructs in the single prostate epithelial cells could inhibit the regeneration into prostatic tubules, and low copy numbers of the lentiviral vector could not be visualized by microscopy. Therefore, the histologic

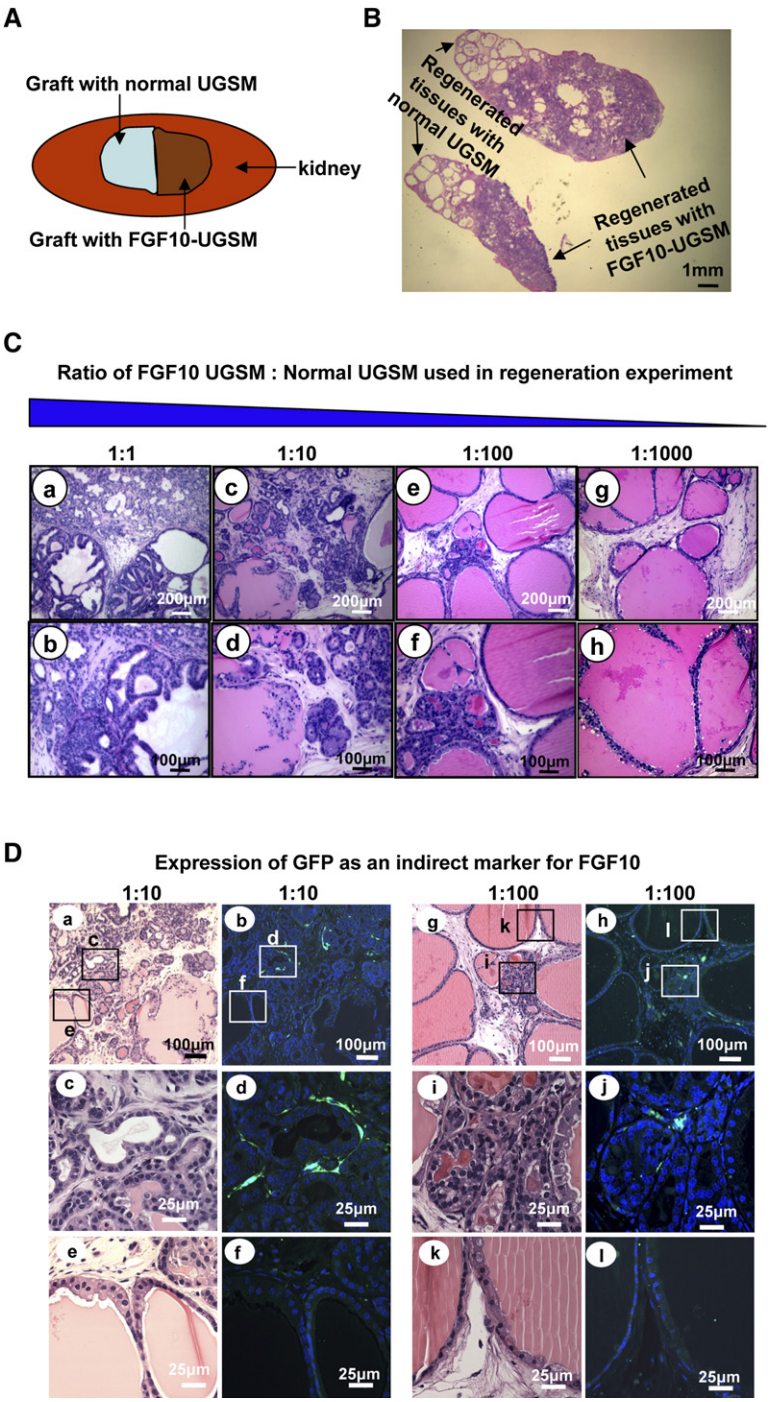

Figure 2. Paracrine FGF10 Signaling Promoted Formation of Multifocal Prostate Cancer Resembling Human PIN or Prostate Cancer and Exerted Its Effects with Regional Specificity

(A) Schematic representation of two adjacent grafts, one with FGF10 UGSM (1×10^5) and a second graft with normal UGSM (1×10^5) both combined with WT epithelium.

(B) Histology of two adjacent grafts revealed normal prostate tubules on one side and well-differentiated prostate cancer on the other side, suggesting localized action of paracrine FGF10.

(C) H&E analysis of regenerated tissue after a logarithmic reduction in the number of FGF10 UGSM revealed evidence of multifocal carcinoma. Cancer was seen in (Ca) and (Cb), PIN was seen adjacent to microinvasive carcinoma in (Cc) and (Cd), multifocal PIN was seen in (Ce) and (Cf), and predominantly normal histology was seen in (Cg) and (Ch).

(D) Expression of FGF10 indirectly detected by anti-GFP staining in areas of hyperplasia.

data gathered in this experiment were on the group of cells expressing intermediate copy numbers of the DN constructs, visualized by the expression of RFP.

Regenerated red cells expressing DN FGFR1 were mostly confined within simple glandular and tubular structures resembling normal prostatic epithelial glands (Figure 3C). These observations were confirmed in four independent experiments. The majority of control RFP or DN FGFR2 red cells were confined within clearly identifiable glands and tubular structures that showed tufting and extension into the glandular lumens, suggestive of epithelial hyperplasia and/or PIN (Figure 3C). The degree of tufting and hypercellularity noted in the DN FGFR2-regenerated glands was less compared to control RFP tissue in some regions. This finding suggests a partial blocking effect resulting from the DN FGFR2 expression, which may be due to nonspecific heterodimerization with FGFR1 (Dailey et al., 2005).

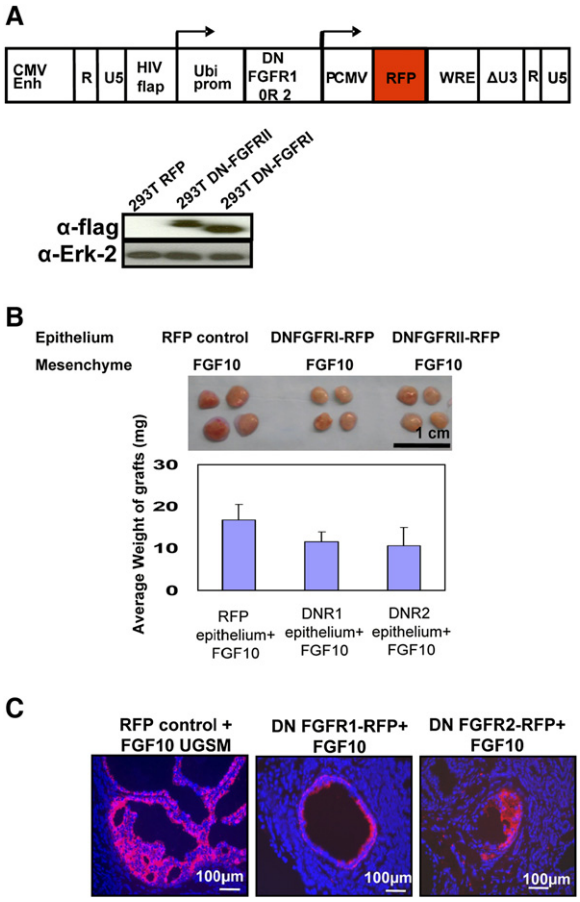

Figure 3. FGF10 Induces Prostate Cancer Predominantly by Activation of FGFR1

(A) The lentivirus FU-CRW vector used for the expression of flag-tagged DN FGFR1 and DN FGF R2. Western blot confirmed the expression of both dominant-negative constructs.

(B) Comparative analysis of graft weights (mean ± SD) regenerated with control vector RFP, DN FGFR1-RFP, or DN FGFR2-RFP and combined with FGF10 (5×10^4) added to WT (5×10^4) UGSM.

(C) Immunofluorescent analysis of grafts regenerated with vector control RFP, DN FGFR1-RFP, or DN FGFR2-RFP. DN FGFR1-RFP-infected tubules showed cells completely confined within simple glandular and tubular structures suggestive of normal prostate epithelium in contrast to RFP or DN FGFR2-RFP-regenerated glands.

Quantitative PCR analysis showed that the expression levels of all other predominant binding partners for FGFR1 (Zhang et al., 2006), in addition to *FGF7* (a homolog of *FGF10*) were not altered significantly (table in Figure S4B) when comparing WT to FGF10 UGSM. These findings rule out the possibility of an FGF10-induced FGF circuitry.

These data suggest that mesenchymal FGF10 predominantly exerted its effects through epithelial FGFR1 and validates previous data demonstrating that activation of FGFR1 plays an important role in neoplastic transformation of prostate epithelium (Freeman et al., 2003). Our data also demonstrate that inhibition of FGFR1 signaling in prostate epithelium reverses the neoplastic phenotype even in a high-FGF10 microenvironment.

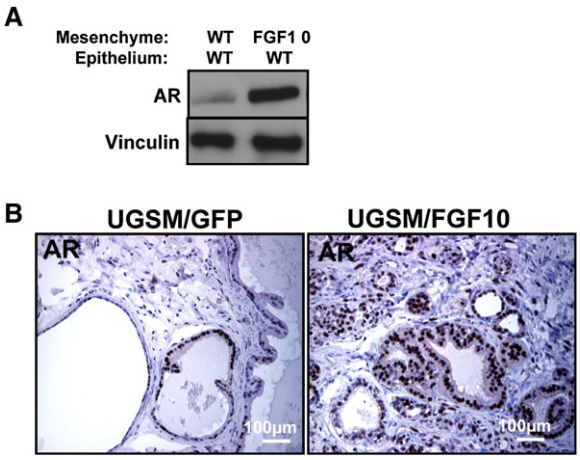

Figure 4. Paracrine FGF10 Resulted in an Increase in Epithelial AR

(A) Western blot revealed a 4-fold increase in expression of AR protein in FGF10- compared to control-regenerated grafts.

(B) Immunohistochemistry confirmed that paracrine FGF10 induced an increase in glandular epithelial AR compared to control-regenerated tissue.

Enhanced Paracrine Mesenchymal FGF10 Leads to an Increase in Epithelial Androgen Receptor

Multiple in vitro but no in vivo studies demonstrate the overexpression or activation of androgen receptor (AR) by fibroblast growth factor peptides. In vitro studies have shown that growth factors such as KGF can stimulate messenger RNA levels of *AR* in the absence of androgens (Planz et al., 2001). IGF-I, EGF, and KGF can activate AR in the absence of androgens, suggesting that these growth factors can directly activate the androgen signaling pathway (Culig et al., 1994).

To examine the effects of paracrine FGF10 on the expression of AR in our model, western blot analysis was performed on protein lysates obtained from regenerated grafts. Densitometry showed a roughly 4-fold increase in AR when comparing FGF10- to control-regenerated grafts (Figure 4A).

Immunohistochemistry was performed to localize the expression of AR. We determined that the majority of epithelial cells in the FGF10 grafts strongly expressed nuclear AR (Figures 4B). The level of AR protein expression was higher in the glandular epithelium of FGF10-regenerated grafts compared to controls, as observed by the relative intensities of AR staining (Figure 4B).

Similar to other steroid hormones, AR undergoes post-translational modifications that can culminate in an increase both in stability and activity of this receptor (Faus and Haendler, 2006). Signaling through growth factor receptors is one mechanism by which these posttranslational modifications can be achieved (Reddy et al., 2006). Quantitative PCR revealed that mRNA levels of *AR*, obtained from epithelia exposed to paracrine FGF10, are not dramatically altered compared to control-regenerated epithelium (data not shown). These results suggest that the FGF10-induced increase in epithelial AR maybe mediated at a posttranslational level.

Paracrine FGF10 Promotes Androgen-Independent Survival and Proliferation of Cancer Cells

Signaling through growth factor receptors can promote androgen-independent growth of prostate cancer cells by amplification of *AR*, an increase in the activation of existing AR, modulation of coactivators/corepressors, and posttranslational modifications that stabilize AR (Feldman and Feldman, 2001).

To assess whether FGF10-induced adenocarcinoma survives following withdrawal of androgen, animals harboring grafts composed of FGF10 or control mesenchyme were castrated and followed for 6 weeks. Histologic analysis of the FGF10 grafts harvested from castrate animals revealed persistence of well-differentiated prostate adenocarcinoma (Figures 5Aa–5Ac). In contrast, in the WT mesenchyme regenerated tissue, there was loss of many epithelia with a remaining, depleted-appearing glandular architecture (Figures 5Ad–5Af). Our results suggest that the FGF10-induced prostate adenocarcinoma cells harbor survival mechanisms that allow proliferation and survival in castrate levels of androgen.

Immunohistochemistry was performed to compare the localization and expression of AR in the intact versus castrate FGF10 grafts (Figure 5B). The glandular tissue of the intact FGF10 grafts expressed high levels of nuclear AR (Figures 5Ba and 5Bb). Castration led to partial cytoplasmic translocation of AR in the FGF10-regenerated tissue (Figures 5Bc and 5Bd). However, partial nuclear localization of AR persisted in the majority of the FGF10 glandular epithelium, and there were foci that continued to harbor strong nuclear expression of AR (Figures 5Bc and 5Bd).

To assess the acute and chronic effects of androgen withdrawal on proliferation and apoptosis in FGF10-regenerated tissue, animals harboring FGF10 mesenchymal grafts were castrated, and grafts were harvested at 1 and 6 weeks. Castrated grafts were half the size of grafts harvested from intact animals at 6 weeks (Figure 5C). We quantified the proliferation index at 6 weeks, and rate of apoptosis at 1 week postcastration using Ki67 immunohistochemistry and TUNEL assays, respectively (Figures S5A and S5B). We counted and averaged the Ki67- or TUNEL-positive epithelia in five high-power microscopic fields. A decrease in proliferation measured by the percentage of Ki67-positive cells (8% in intact versus 4% in castrate), which did not reach statistical significance, and a statistical significant increase in apoptosis measured by the percentage of TUNEL-positive cells (0.8% in intact versus 1.6% in castrate) was seen upon castration (Figures S5A and S5B).

Decrease in the size of the grafts, increase in apoptosis, and decrease in proliferation upon castration suggest that a subset of the FGF10-induced adenocarcinoma remains dependent on androgen hormone. Persistence of the remaining FGF10-induced prostate adenocarcinoma cells and Ki67 staining suggests that paracrine FGF10 signaling can promote survival and proliferation of these cells in castrate levels of androgen. The dramatic increase in AR

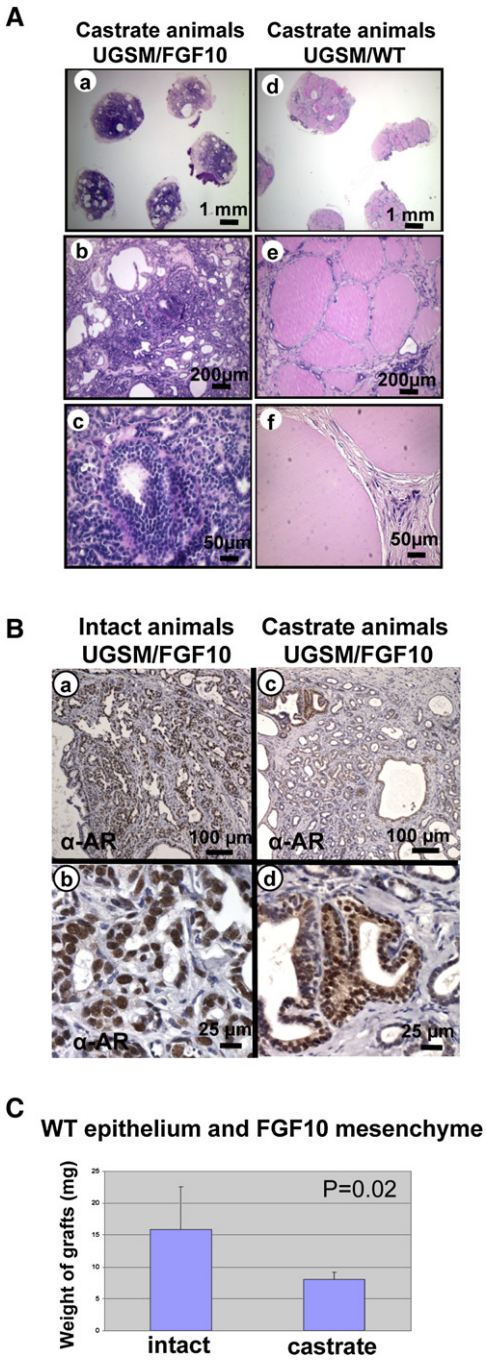

Figure 5. Paracrine FGF10 Promoted Androgen-Independent Survival of a Subset of Prostate Adenocarcinoma

(A) Histology of the FGF10 and WT mesenchyme regenerated grafts harvested from castrated animals. Loss of many epithelia was observed in WT grafts. In contrast, persistence of adenocarcinoma cells was noted in all five FGF10-regenerated specimens.

(B) Immunohistochemical localization of AR in FGF10 grafts obtained from intact and castrated animals. Castration led to partial cytoplasmic transport of AR in castrate (Bc and Bd) compared to intact (Ba and Bb) grafts. Partial nuclear localization of AR persisted despite castration in the FGF10-regenerated tissue (Bc and Bd).

(C) Comparative analysis of weight (mean ± SD) of grafts harvested from intact and castrate animals.

induced by paracrine FGF10 and subsequent hypersensitivity to residual castrate levels of androgens may be one survival strategy used by the surviving cancer cells after castration. Androgen-independent activation of AR by paracrine FGF10 may be an alternate mechanism leading to androgen-independent survival of a subset of the FGF10-induced adenocarcinoma.

A Subset of FGF10-Induced PIN or Adenocarcinoma Is Serially Transplantable

While chronic signaling through an oncogenic pathway is essential for maintaining transformation in some malignancies, cell-autonomous alterations can be sufficient to bypass this continual dependence in other cancer models (Weinstein, 2002). We assessed whether transformation of epithelia exposed to FGF10 would evade or remain dependent on chronic paracrine signaling by this growth factor and asked whether the FGF10-induced adenocarcinoma was serially transplantable. Prostate epithelium from DS red transgenic animals were recombined with FGF10-GFP UGSM and placed in the regeneration system. DS red transgenic animals were used as they express the red fluorescent protein variant DS Red, providing a fluorescent marker for the epithelia. Grafts were harvested following 8 weeks of regeneration, minced, and digested into single cells.

Dilution of FGF10-UGSM cells by a factor of 1000 would lead to formation of normal tubules in this regeneration system (Figure 2C). DS red dissociated single cells (2×10^4) harvested from FGF10-regenerated grafts were combined with WT epithelium (2×10^4) and an excess of WT mesenchyme such that the number of FGF10-expressing mesenchymal cells would be diluted by a factor of 1000. These cells were engrafted as a secondary tumor. After 8 weeks of regeneration, histologic analysis revealed areas of WT epithelium adjacent to hyperplastic foci of cells with uniform epithelial tufting, crowding, and nuclear atypia (Figures S6Aa–S6Ac). Immunofluorescent microscopy revealed WT and red tubules forming double-layered large tubules with normal architecture adjacent to red clusters of glands filled with several layers of tufted epithelial cells, reminiscent of PIN (Figures S6Ad–S6Af). This observation suggested that the FGF10-induced PIN could persist in an FGF10-low microenvironment.

DS red dissociated single cells harvested from FGF10-regenerated grafts were FACS sorted (R1), assuring exclusion of single or doublets of GFP-positive cells (R2 + R3) (Figure 6A). DS red sorted cells (3×10^4) were either recombined with WT epithelia (7×10^4) as helper cells, or engrafted alone with WT UGSM cells (10^5) as a secondary tumor in the regeneration system. Histologic analysis of grafts with added helper cells revealed multiple normal tubules, in addition to areas demonstrating cellular tufting, crowding, and few foci with crowded microglandular structures containing cells with atypical nuclear features and higher nuclear-to-cytoplasmic ratios (Figures 6Aa and 6Ab). Immunofluorescent microscopic evaluation of this regenerated tissue revealed formation of some double-layered large red tubules resembling normal glands (Figures 6Ba and 6Bb), in addition to other areas demonstrating small clusters of red tubules reminiscent of well-differentiated adenocarcinoma (Figure 6Bc and 6Bd).

Our findings suggest that an 8 week exposure to paracrine FGF10 may induce a subset of epithelial cells to continuously form abnormal epithelial structures, architecturally ranging from hyperplasia to well-differentiated adenocarcinoma, even in low levels of this growth factor. To test whether the FGF10-induced adenocarcinoma is serially transplantable, we dissociated secondary grafts into single cells and retransplanted them into a tertiary graft (Figure S6B). In these tertiary grafts, similar to the primary and secondary tumors, we observed abnormal epithelial structures architecturally ranging from epithelial hyperplasia to well-differentiated adenocarcinoma, suggesting that a subset of FGF10-induced PIN/adenocarcinoma is serially transplantable (Figure S6B). The rate of proliferation of the transplanted secondary and tertiary tumors was found to be similar to the primary FGF10 grafts and significantly more than normal regenerated tissue assessed and quantified by Ki67 staining (Figure S7).

To ascertain possible mechanisms that could account for this sustained oncogenic phenotype, in low levels of FGF10, transplanted DS red regenerated tissue (without helper cells) were evaluated for phosphotyrosine activation in secondary and tertiary tumors. Immunohistochemical analysis of the transplanted tissue with pan-phosphotyrosine antibody revealed strong phosphotyrosine activation in cancerous regenerated glands (Figures 6Cc, 6Cd, 6Cg, and 6Ch; Figure S8B). In these histologic specimens, the absence of GFP staining further confirmed the exclusion of exogenous growth factor-expressing UGSM cells (Figures 6Cb and 6Cf). Regenerated tissue with normal UGSM was used as a negative control, and cancerous tissue with FGF10 UGSM was used as positive control in assessing phosphotyrosine activity (Figure S8B). Sustained nuclear localization of AR was seen in secondary and tertiary transplanted regenerated tissue, demonstrating sustained activation of the AR machinery (Figures 6Da and 6Db; Figure S8A).

Cooperation between Mesenchymal FGF10 and Cell-Autonomous AKT Leads to High-Grade Carcinoma

We sought to evaluate the biological consequences of combining two events in naive prostate epithelial cells, "outside-in" signaling through mesenchymal FGF10 and cell-autonomous expression of activated AKT. We had previously shown that chronic activated epithelial AKT could lead to the formation of PIN, while the combination of epithelial AKT and AR would lead to the formation of carcinoma (Xin et al., 2006). In this model, paracrine FGF10 signaling led to an increase in epithelial AR. We asked whether paracrine FGF10 signaling could synergize with cell-autonomous activated AKT.

Prostate single cells were infected with control vector or activated AKT and combined with either FGF 10 expressing UGSM or vector control UGSM and placed in the regeneration system. Grafts were harvested after 7 weeks

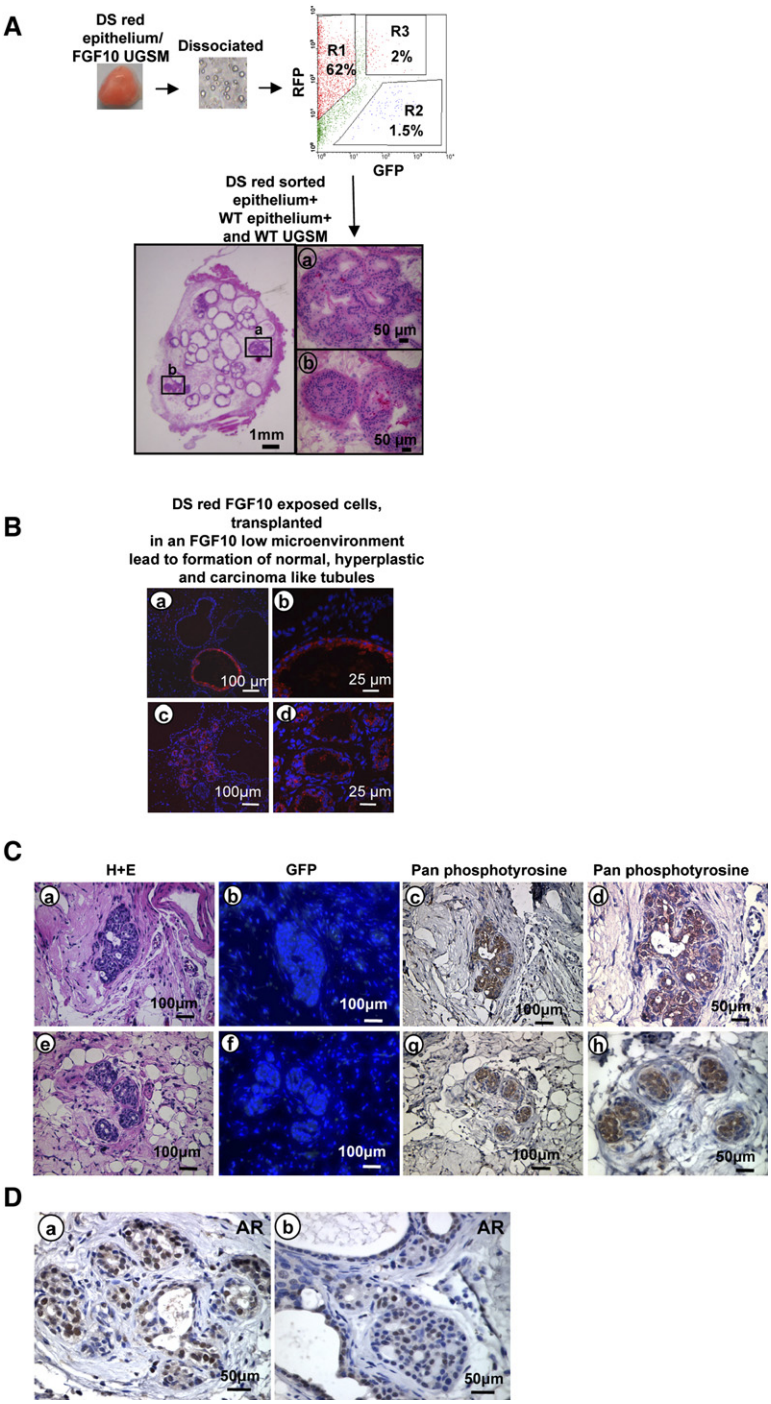

Figure 6. Serial Transplantation of a Subset of FGF10 Induced Adenocarcinoma

(A) Schematic representation of transplantation experiments and histology of regenerated tubules.

(B) Immunofluorescent analysis of regenerated tissue revealed formation of many WT and some red epithelial glands with a single cell layer resembling normal tubules (Ba and Bb), and multiple small red tubules adjacent to normal-appearing WT glands reminiscent of well-differentiated adenocarcinoma (Bc and Bd).

(C) Histologic evaluation of transplanted tissue specimens revealed evidence of adenocarcinoma (Ca and Ce) and absence of contaminating FGF10-expressing stromal cells demonstrated by lack of GFP staining (Cb and Cf). The cancerous regenerated tissue revealed strong phosphotyrosine activation after withdrawal of retrovirally infected FGF10 UGSM cells (Cc, Cd, Cg, and Ch).

(D) Persistent strong nuclear localization of AR was observed in cancerous areas of the transplanted regenerated grafts (Da and Db).

and weighed (Figure 7A), and the histology was evaluated (Figures 7Ba–7Bf). Addition of epithelial AKT to mesenchymal FGF 10 more than doubled the size of the grafts as compared to grafts with epithelial AKT alone (Figure 7A). The combination of AKT and FGF10 resulted in grafts that were six times the weight of grafts with FGF10 alone (Figure 7A). Histologic analysis of the 3/3 regenerated grafts revealed areas of poorly differentiated adenocarcinoma with mesenchymal FGF10 and epithelial AKT, defined by sheets of atypical cells with almost complete loss of glandular architecture (Figures 7Bc and 7Bf; Figure S9). Mesenchymal FGF10 led to the development of well-differentiated adenocarcinoma (Figures 7Ba and 7Bd), and epithelial AKT alone led to PIN defined by stratification of epithelial cells with nuclear atypia confined within glandular structures (Figures 7Bb and 7Be). Expression of epithelial phospho-AKT was confirmed using immunohistochemistry (Figures 7Bh and 7Bi). Stromal

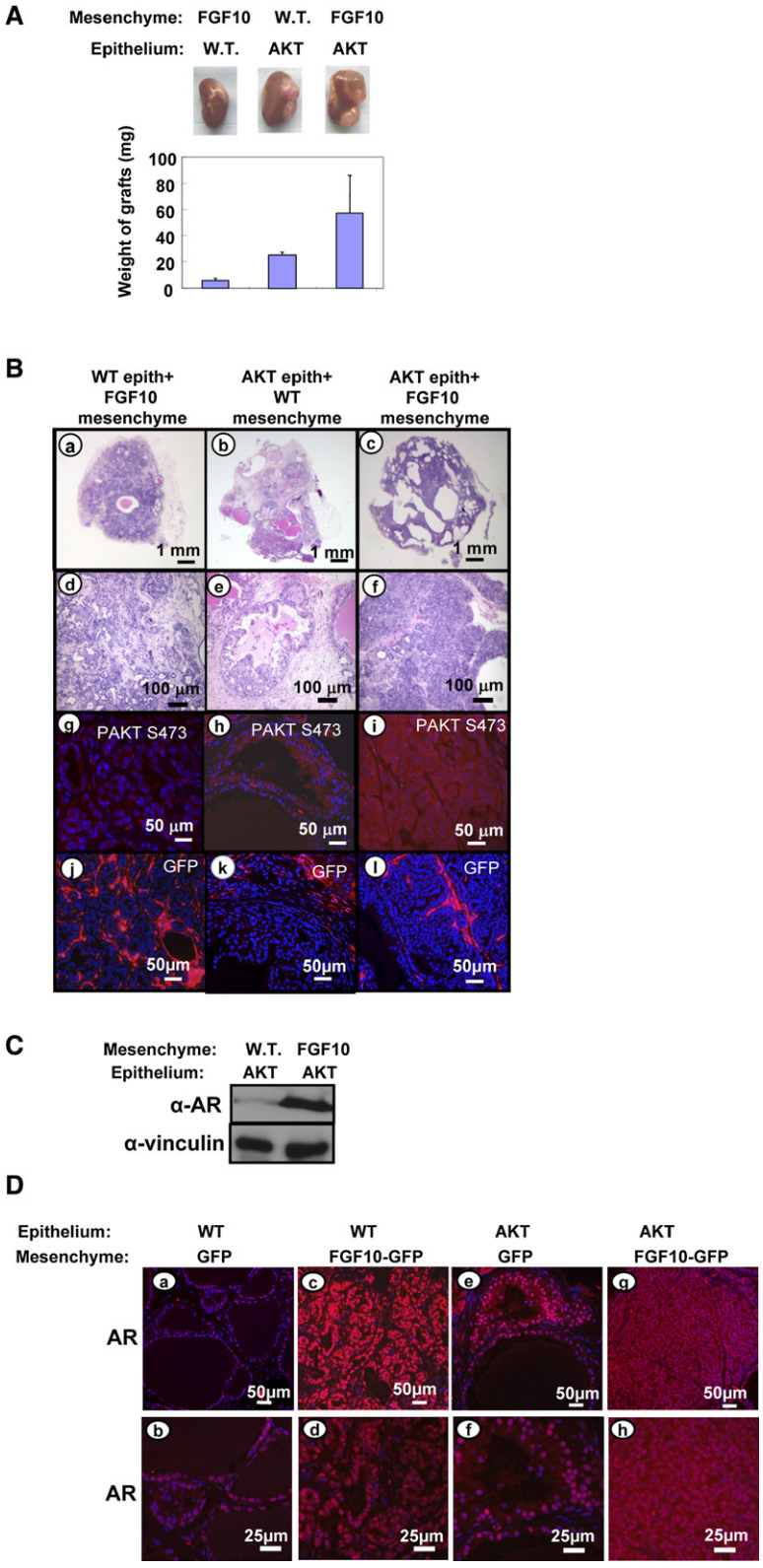

Figure 7. Mesenchymal FGF10 Synergized with Cell-Autonomous AKT Leading to a Progressive Cancer Phenotype and a Dramatic Increase in Epithelial AR

(A) Transilluminating images and comparative weight (mean ± SD) of grafts derived from WT epithelium with FGF10 UGSM, AKT epithelium with WT UGSM and AKT epithelium with FGF10 UGSM.

(B) H&E staining for the regenerated tissue derived from WT epithelium with FGF10 UGSM (Ba and Bd), AKT epithelium with WT UGSM (Bb and Be) and AKT epithelium with FGF10 UGSM (Bc and Bf). Immunohistochemical analysis of the expression phospho-AKT (Bg–Bi) and GFP (Bj–Bl).

(C) Western blot analysis with AR antibody confirmed the increase in AR in the presence of mesenchymal FGF10. Vinculin used as loading control.

(D) Immunofluorescence detection of AR revealed that FGF10 mesenchyme in combination with WT or AKT activated epithelium could lead to an increase in expression of epithelial AR compared to controls.

expression of FGF10-GFP or GFP was confirmed by immunohistochemical detection of GFP (Figures 7Bj–7Bl). Our data demonstrate synergy between paracrine FGF10 signaling and cell-autonomous AKT, implicating the importance of cooperation between stromal and epithelial perturbations in malignant transformation.

To ascertain the possible mechanisms for cooperation between paracrine mesenchymal FGF10 and cell-autonomous AKT, regenerated grafts were lysed for western blot analysis (Figure 7C). We had previously observed a 4-fold increase in the expression of AR comparing FGF10 to control grafts (Figure 4A). Similarly, densitometry on western blots showed roughly an 8-fold increase in AR protein when comparing grafts composed of epithelial AKT combined with mesenchymal FGF10 to grafts composed of epithelial AKT alone (Figure 7C). Immunohistochemistry confirmed that AR was mainly overexpressed in the epithelial compartment (Figures 7Da and 7Db compared to 7Dc and 7Dd and Figures 7De and 7Df compared to 7Dg and 7Dh).

These data indicate that paracrine FGF10 signaling leads to an increase in epithelial AR, and this secondary event can cooperate with activated epithelial AKT, leading to a progressive cancer phenotype.

DISCUSSION

Historically, essential growth factors have proven to be oncogenic in multiple tumor models (Kris et al., 1985). For example, platelet-derived growth factor, an essential peptide for wound healing, was one of the first described growth factor oncogenes (Doolittle et al., 1983). We have demonstrated that enhanced expression of stromal FGF10, an essential gene for prostate development, is sufficient for the formation of multifocal adenocarcinoma concomitant with an increase in epithelial AR in an in vivo prostate cancer model.

Similar to FGF10, AR is essential for the development of the prostate (Cunha and Lung, 1978). We show that enhanced expression of stromal FGF10 is sufficient to increase levels of AR protein in both naive and activated AKT prostate epithelium. Interestingly, in our study, expression of additional AR in WT epithelium using lentiviral delivery vectors in combination with mesenchymal FGF10 led to no discernable histologic difference compared to mesenchymal FGF10-regenerated grafts (Figures S10A and S10B). Developmental studies using in vitro organ culture systems of *FGF10* null prostate demonstrate that addition of exogenous FGF10 can induce branching morphogenesis similar to the addition of testosterone, while addition of both FGF10 and testosterone do not provide further synergistic effects (Thomson and Cunha, 1999). Our findings concur with previous observations and suggest that paracrine FGF10 signaling can promote activation of AR. An increase in AR protein may be one mechanism by which this overactivation is achieved.

Amplification of the *AR* gene has been reported in up to 30% of human prostate cancers and is thought to be an important mechanism for formation of androgen independence (Chen et al., 2004; Feldman and Feldman, 2001). Perturbations in the growth factor regulatory loops are associated with progression to a more aggressive cancer phenotype leading to androgen-independent metastatic disease (Culig et al., 2000, 2002; Scher et al., 1995). In our model, survival of a subset of the FGF10-induced prostate adenocarcinoma cells, concomitant with partial nuclear localization of AR in the castrate tumors, suggests activation of AR signaling axis by paracrine mesenchymal FGF10 in castrate levels of androgen.

Transformed cells, such as Bcr-Abl-induced leukemia (Huettner et al., 2000) or ras-induced melanoma (Chin et al., 1999), are found to be "addicted" to oncogenic signals, such that removal of the activating signal can lead to regression of the cancer phenotype (Weinstein, 2002). It is conceivable that a subset of cells exposed to an oncogene may undergo subsequent genetic alterations allowing them to evade chronic dependence on the initial growth-promoting activated pathway (Weinstein, 2002). This phenomenon is seen in a subpopulation of c-*myc*-induced mammary carcinoma cells that can continue to grow in a myc-independent manner after downregulation of this oncogene (Boxer et al., 2004). Formation of PIN or adenocarcinoma in transplanted epithelia, previously exposed to high levels of FGF10, suggests a possible "hit and run" mechanism for the paracrine FGF10-induced epithelial alterations. Persistence of pan-phosphotyrosine kinase activity and sustained nuclear localization of AR in this subset of transplanted cancerous tissue suggests intrinsic genetic alterations, resulting in survival and growth of this subpopulation of cells in low levels of FGF10. The nongenotropic activity of AR has been linked to activation of several tyrosine kinases including the Src, PI3 kinase (phosphoinositide 3- kinase), and MAPK kinase (mitogen-activated protein kinase) family receptors (Kousteni et al., 2001; Sun et al., 2003). Conversely, activation of protein tyrosine kinases can lead to activation of the AR (Feldman and Feldman, 2001). Either of these mechanisms, in conjunction or solely, could account for the sustained cancerous phenotype noted in the transplanted grafts.

Cancer progression can result from the accumulation of multiple cooperative genetic events, a concept that has been demonstrated in three recent prostate cancer models (Gao et al., 2006; Xin et al., 2006; Zhong et al., 2006). Cooperation between autocrine FGFR signaling and the PI3 Kinase pathway was shown in an in vivo transgenic animal model in which loss of PTEN and overexpression of FGF8b in the epithelium led to poorly differentiated adenocarcinoma (Zhong et al., 2006). We had previously shown synergy between epithelial AR and AKT resulting in adenocarcinoma that resists the effects of androgen ablation (Xin et al., 2006). Loss of PTEN and Nkx3.1 is another mechanism that can promote androgen-independent prostate carcinoma (Gao et al., 2006). Our study emphasizes synergy between a paracrine growth factor, FGF10, and epithelial cell-autonomous activated AKT. This model emphasizes the importance of stromal paracrine and epithelial cell-autonomous signals leading to the development of poorly differentiated disease.

These data suggest the importance of targeting the growth factor receptor signaling axis through either inhibition of paracrine factors or direct inhibition of growth factor receptors, in conjunction with other therapeutic strategies, such as androgen ablation used in treating

prostate cancer. Targeting growth factor signaling cascades similar to fibroblast growth factors may also delay emergence of androgen hormone independence, which poses the largest clinical challenge in the treatment of prostate cancer.

EXPERIMENTAL PROCEDURES

Plasmids

cDNA encoding *FGF10* was procured by RT-PCR, from NIH 3T3 cells, and cloned into the EcoRI site of MSCV-IRES-GFP (MSCV, murine stem cell virus; IRES, internal ribosomal entry site) (Hawley et al., 1994). *DN FGFR1* and *DN FGFR2* (Li et al., 1994) were flag tagged and subcloned into the EcoRI cloning site of FU-CRW lentiviral expression vector. FU-CRW is a vector derived from FUGW (Xin et al., 2006). In the FU-CRW vector the *GFP* coding sequence of FUGW vector was substituted with a *CMV*-driven *RFP* expression cassette. Myristoylated human *AKT1* was subcloned into the EcoRI site of FU-CRW lentiviral expression vector.

Prostate Regeneration and Prostate Epithelial Viral Infections

The details of the regeneration process and viral infection of epithelial cells have been explained previously (Xin et al., 2003). Housing, maintenance, and all surgical procedures were undertaken in compliance with the regulations of the Division of Laboratory Animal Medicine of the University of California, Los Angeles. All experimental procedures were approved by the Division of Laboratory Animal Medicine of the University of California, Los Angeles. Viral preparation procedures were performed under University of California, Los Angeles, safety regulations for lentivirus usage. Retrovirus and lentivirus were made as described previously (Wong et al., 2004; Xin et al., 2003, 2006).

Immunohistochemistry

Grafts were fixed in buffered formalin 10% and placed in 70% ethanol as described previously (Xin et al., 2003, 2006). Sections (4 μm) were made and stained with hematoxylin and eosin (H&E) or with antibodies against CK5 (AF138, Abcam), P63 (sc-8431, Santa Cruz Biotechnology), E-cadherin (610-182, Transduction), anti-AR (sc-816, Santa Cruz Biotechnology), P AKT (3787, Cell Signaling), GFP (mouse monoclonal clone 3C2-G2 produced in O.N.W.'s labs), anti-Brdu (51-75512 PharMingen), pan-phosphotyrosine (Upstate), CK8 (MMS-162P Covance), and Ki67 (Vector) antibodies. For visualization of CK5, E-cadherin, AR, pAKT biotinylated anti-mouse IgG (RO627, Vector Biotechnology), and biotinylated anti-rabbit IgG (ab6720-1, Abcam) secondary antibodies were used. Histologic sections were visualized with fluorescent microscopy and counterstained with DAPI (Vector Laboratories).

Western Blot

Grafts and cells were manually lysed in RIPA buffer composed of 50 mM Tris-HCl (pH 8.0), 150 mM NaCl, 0.1% SDS, 0.5% SD, 1% NP-40, 1 mM EDTA, 1 mM PMSF, 25 mM NaF, cocktail protease inhibitors (Roche), and phosphatase inhibitor 1 and 2 (Sigma). Secreted FGF10 protein was collected and precipitated from a 48 hr low serum cultured media collected from UGSM cells expressing FGF10 at a 4:1 ratio with 50% TCA (trichlor acetic acid), centrifuged, pelleted, washed with acetone, air dried, and resuspended with 2× SDS lysis buffer. pH was adjusted with 10 M NaOH. Protein lysates (40–100 μg) were separated by SDS-PAGE followed by western blot analysis using AR (sc-816, Santa Cruz Biotechnology), FGF10 (sc-Santa Cruz Biotechnology), Vinculin (Sigma), anti-flag (Sigma), and Erk2 (sc-154, Santa Cruz Biotechnology) antibodies. Quantification of the western blot data was performed using the NIH ImageJ program (http://rsb.info.nih.gov/ij/).

Quantitative RT-PCR

Quantitative RT-PCR was performed using an ABI 7700 Real Time PCR System. Primers are listed in the table in Figure S4A. All primers span at least one intron. Standard curves of murine placenta cDNA were run for each primer pair, and the amount of target gene was normalized to the amount of actin.

Supplemental Data

The Supplemental Data include ten supplemental figures and can be found with this article online at http://www.cancercell.org/cgi/content/full/12/6/572/DC1/.

ACKNOWLEDGMENTS

We thank Ms. Barbara Anderson for her help in preparation of this manuscript and Ms. Donghui Cheng for her help in FACS sorting cells. S.M. has been supported by grants from NICHD-ABOG Reproductive Scientist Developmental Program 5K12HD00849-18 and NIH/National Cancer Institute, Clinical Scientist Training in Cancer Gene Medicine, K12-CA076905-09. L.X. is supported by a NIH Pathway to Independence Award 1K99CA125937 and a training grant from the California Institute for Regenerative Medicine. D.J.M. is funded by a National Institutes of Health (NIH) fellowship. H.W. is supported by NIH grant RO1 CA107166 and an Army Medical Research grant W81XWH-05-1-0542. M.A.T. is a Scholar of the Leukemia and Lymphoma Society and is supported by NIH grants R01CA90571 and R01CA107300, and California Institute for Regenerative Medicine (CIRM) grant RS1-00313. O.N.W. is an investigator of the Howard Hughes Medical Institute.

Received: February 8, 2007
Revised: July 16, 2007
Accepted: November 1, 2007
Published: December 10, 2007

REFERENCES

Bhowmick, N.A., Chytil, A., Plieth, D., Gorska, A.E., Dumont, N., Shappell, S., Washington, M.K., Neilson, E.G., and Moses, H.L. (2004a). TGF-beta signaling in fibroblasts modulates the oncogenic potential of adjacent epithelia. Science *303*, 848–851.

Bhowmick, N.A., Neilson, E.G., and Moses, H.L. (2004b). Stromal fibroblasts in cancer initiation and progression. Nature *432*, 332–337.

Bostwick, D.G., and Foster, C.S. (1999). Predictive factors in prostate cancer: Current concepts from the 1999 College of American Pathologists Conference on Solid Tumor Prognostic Factors and the 1999 World Health Organization Second International Consultation on Prostate Cancer. Semin. Urol. Oncol. *17*, 222–272.

Boxer, R.B., Jang, J.W., Sintasath, L., and Chodosh, L.A. (2004). Lack of sustained regression of c-MYC-induced mammary adenocarcinomas following brief or prolonged MYC inactivation. Cancer Cell *6*, 577–586.

Chen, C.D., Welsbie, D.S., Tran, C., Baek, S.H., Chen, R., Vessella, R., Rosenfeld, M.G., and Sawyers, C.L. (2004). Molecular determinants of resistance to antiandrogen therapy. Nat. Med. *10*, 33–39.

Cheng, N., Bhowmick, N.A., Chytil, A., Gorksa, A.E., Brown, K.A., Muraoka, R., Arteaga, C.L., Neilson, E.G., Hayward, S.W., and Moses, H.L. (2005). Loss of TGF-beta type II receptor in fibroblasts promotes mammary carcinoma growth and invasion through upregulation of TGF-alpha-, MSP- and HGF-mediated signaling networks. Oncogene *24*, 5053–5068.

Chin, L., Tam, A., Pomerantz, J., Wong, M., Holash, J., Bardeesy, N., Shen, Q., O'Hagan, R., Pantginis, J., Zhou, H., et al. (1999). Essential role for oncogenic Ras in tumour maintenance. Nature *400*, 468–472.

Culig, Z., Hobisch, A., Cronauer, M.V., Radmayr, C., Trapman, J., Hittmair, A., Bartsch, G., and Klocker, H. (1994). Androgen receptor activation in prostatic tumor cell lines by insulin-like growth factor-I,

keratinocyte growth factor, and epidermal growth factor. Cancer Res. *54*, 5474–5478.

Culig, Z., Hobisch, A., Bartsch, G., and Klocker, H. (2000). Androgen receptor—An update of mechanisms of action in prostate cancer. Urol. Res. *28*, 211–219.

Culig, Z., Klocker, H., Bartsch, G., and Hobisch, A. (2002). Androgen receptors in prostate cancer. Endocr. Relat. Cancer *9*, 155–170.

Cunha, G.R., and Lung, B. (1978). The possible influence of temporal factors in androgenic responsiveness of urogenital tissue recombinants from wild-type and androgen-insensitive (Tfm) mice. J. Exp. Zool. *205*, 181–193.

Dailey, L., Ambrosetti, D., Mansukhani, A., and Basilico, C. (2005). Mechanisms underlying differential responses to FGF signaling. Cytokine Growth Factor Rev. *16*, 233–247.

Das, D., Shah, R.B., and Imperiale, M.J. (2004). Detection and expression of human BK virus sequences in neoplastic prostate tissues. Oncogene *23*, 7031–7046.

Dong, B., Kim, S., Hong, S., Das Gupta, J., Malathi, K., Klein, E.A., Ganem, D., Derisi, J.L., Chow, S.A., and Silverman, R.H. (2007). An infectious retrovirus susceptible to an IFN antiviral pathway from human prostate tumors. Proc. Natl. Acad. Sci. USA *104*, 1655–1660.

Donjacour, A.A., Thomson, A.A., and Cunha, G.R. (2003). FGF-10 plays an essential role in the growth of the fetal prostate. Dev. Biol. *261*, 39–54.

Doolittle, R.F., Hunkapiller, M.W., Hood, L.E., Devare, S.G., Robbins, K.C., Aaronson, S.A., and Antoniades, H.N. (1983). Simian sarcoma virus onc gene, v-sis, is derived from the gene (or genes) encoding a platelet-derived growth factor. Science *221*, 275–277.

Faus, H., and Haendler, B. (2006). Post-translational modifications of steroid receptors. Biomed. Pharmacother. *60*, 520–528.

Feldman, B.J., and Feldman, D. (2001). The development of androgen-independent prostate cancer. Nat. Rev. Cancer *1*, 34–45.

Feng, S., Wang, F., Matsubara, A., Kan, M., and McKeehan, W.L. (1997). Fibroblast growth factor receptor 2 limits and receptor 1 accelerates tumorigenicity of prostate epithelial cells. Cancer Res. *57*, 5369–5378.

Foster, B.A., Evangelou, A., Gingrich, J.R., Kaplan, P.J., DeMayo, F., and Greenberg, N.M. (2002). Enforced expression of FGF-7 promotes epithelial hyperplasia whereas a dominant negative FGFR2iiib promotes the emergence of neuroendocrine phenotype in prostate glands of transgenic mice. Differentiation *70*, 624–632.

Freeman, K.W., Welm, B.E., Gangula, R.D., Rosen, J.M., Ittmann, M., Greenberg, N.M., and Spencer, D.M. (2003). Inducible prostate intraepithelial neoplasia with reversible hyperplasia in conditional FGFR1-expressing mice. Cancer Res. *63*, 8256–8263.

Gao, H., Ouyang, X., Banach-Petrosky, W.A., Gerald, W.L., Shen, M.M., and Abate-Shen, C. (2006). Combinatorial activities of Akt and B-Raf/Erk signaling in a mouse model of androgen-independent prostate cancer. Proc. Natl. Acad. Sci. USA *103*, 14477–14482.

Greenberg, N.M., DeMayo, F., Finegold, M.J., Medina, D., Tilley, W.D., Aspinall, J.O., Cunha, G.R., Donjacour, A.A., Matusik, R.J., and Rosen, J.M. (1995). Prostate cancer in a transgenic mouse. Proc. Natl. Acad. Sci. USA *92*, 3439–3443.

Harding, M.A., and Theodorescu, D. (2000). Prostate tumor progression and prognosis. Interplay of tumor and host factors. Urol. Oncol. *5*, 258–264.

Hawley, R.G., Lieu, F.H., Fong, A.Z., and Hawley, T.S. (1994). Versatile retroviral vectors for potential use in gene therapy. Gene Ther. *1*, 136–138.

Hill, R., Song, Y., Cardiff, R.D., and Van Dyke, T. (2005). Selective evolution of stromal mesenchyme with p53 loss in response to epithelial tumorigenesis. Cell *123*, 1001–1011.

Huettner, C.S., Zhang, P., Van Etten, R.A., and Tenen, D.G. (2000). Reversibility of acute B-cell leukaemia induced by BCR-ABL1. Nat. Genet. *24*, 57–60.

Huss, W.J., Barrios, R.J., Foster, B.A., and Greenberg, N.M. (2003). Differential expression of specific FGF ligand and receptor isoforms during angiogenesis associated with prostate cancer progression. Prostate *54*, 8–16.

Kalluri, R., and Zeisberg, M. (2006). Fibroblasts in cancer. Nat. Rev. Cancer *6*, 392–401.

Kousteni, S., Bellido, T., Plotkin, L.I., O'Brien, C.A., Bodenner, D.L., Han, L., Han, K., DiGregorio, G.B., Katzenellenbogen, J.A., Katzenellenbogen, B.S., et al. (2001). Nongenotropic, sex-nonspecific signaling through the estrogen or androgen receptors: Dissociation from transcriptional activity. Cell *104*, 719–730.

Kris, R.M., Libermann, T.A., Avivi, A., and Schlessinger, J. (1985). Growth factors, growth-factor receptors and oncogenes. Nat. Biotechnol. *3*, 135–140.

Kwabi-Addo, B., Ozen, M., and Ittmann, M. (2004). The role of fibroblast growth factors and their receptors in prostate cancer. Endocr. Relat. Cancer *11*, 709–724.

Li, Y., Basilico, C., and Mansukhani, A. (1994). Cell transformation by fibroblast growth factors can be suppressed by truncated fibroblast growth factor receptors. Mol. Cell. Biol. *14*, 7660–7669.

Lin, Y., Liu, G., Zhang, Y., Hu, Y.P., Yu, K., Lin, C., McKeehan, K., Xuan, J.W., Ornitz, D.M., Shen, M.M., et al. (2007). Fibroblast growth factor receptor 2 tyrosine kinase is required for prostatic morphogenesis and the acquisition of strict androgen dependency for adult tissue homeostasis. Development *134*, 723–734.

Lu, W., Luo, Y., Kan, M., and McKeehan, W.L. (1999). Fibroblast growth factor-10. A second candidate stromal to epithelial cell andromedin in prostate. J. Biol. Chem. *274*, 12827–12834.

Majumder, P.K., Yeh, J.J., George, D.J., Febbo, P.G., Kum, J., Xue, Q., Bikoff, R., Ma, H., Kantoff, P.W., Golub, T.R., et al. (2003). Prostate intraepithelial neoplasia induced by prostate restricted Akt activation: The MPAKT model. Proc. Natl. Acad. Sci. USA *100*, 7841–7846.

Matsubara, A., Kan, M., Feng, S., and McKeehan, W.L. (1998). Inhibition of growth of malignant rat prostate tumor cells by restoration of fibroblast growth factor receptor 2. Cancer Res. *58*, 1509–1514.

Nakano, K., Fukabori, Y., Itoh, N., Lu, W., Kan, M., McKeehan, W.L., and Yamanaka, H. (1999). Androgen-stimulated human prostate epithelial growth mediated by stromal-derived fibroblast growth factor-10. Endocr. J. *46*, 405–413.

Planz, B., Wang, Q., Kirley, S.D., Marberger, M., and McDougal, W.S. (2001). Regulation of keratinocyte growth factor receptor and androgen receptor in epithelial cells of the human prostate. J. Urol. *166*, 678–683.

Powers, C.J., McLeskey, S.W., and Wellstein, A. (2000). Fibroblast growth factors, their receptors and signaling. Endocr. Relat. Cancer *7*, 165–197.

Reddy, G.P., Barrack, E.R., Dou, Q.P., Menon, M., Pelley, R., Sarkar, F.H., and Sheng, S. (2006). Regulatory processes affecting androgen receptor expression, stability, and function: Potential targets to treat hormone-refractory prostate cancer. J. Cell. Biochem. *98*, 1408–1423.

Sahadevan, K., Darby, S., Leung, H., Mathers, M., Robson, C., and Gnanapragasam, V. (2007). Selective over-expression of fibroblast growth factor receptors 1 and 4 in clinical prostate cancer. J. Pathol. *213*, 82–90.

Scher, H.I., Sarkis, A., Reuter, V., Cohen, D., Netto, G., Petrylak, D., Lianes, P., Fuks, Z., Mendelsohn, J., and Cordon-Cardo, C. (1995). Changing pattern of expression of the epidermal growth factor receptor and transforming growth factor alpha in the progression of prostatic neoplasms. Clin. Cancer Res. *1*, 545–550.

Seftor, E.A., Brown, K.M., Chin, L., Kirschmann, D.A., Wheaton, W.W., Protopopov, A., Feng, B., Balagurunathan, Y., Trent, J.M., Nickoloff,

B.J., et al. (2005). Epigenetic transdifferentiation of normal melanocytes by a metastatic melanoma microenvironment. Cancer Res. *65*, 10164–10169.

Shappell, S.B., Thomas, G.V., Roberts, R.L., Herbert, R., Ittmann, M.M., Rubin, M.A., Humphrey, P.A., Sundberg, J.P., Rozengurt, N., Barrios, R., et al. (2004). Prostate pathology of genetically engineered mice: Definitions and classification. The consensus report from the Bar Harbor meeting of the Mouse Models of Human Cancer Consortium Prostate Pathology Committee. Cancer Res. *64*, 2270–2305.

Sun, M., Yang, L., Feldman, R.I., Sun, X.M., Bhalla, K.N., Jove, R., Nicosia, S.V., and Cheng, J.Q. (2003). Activation of phosphatidylinositol 3-kinase/Akt pathway by androgen through interaction of p85alpha, androgen receptor, and Src. J. Biol. Chem. *278*, 42992–43000.

Thomson, A.A., and Cunha, G.R. (1999). Prostatic growth and development are regulated by FGF10. Development *126*, 3693–3701.

Vukovic, B., Park, P.C., Al-Maghrabi, J., Beheshti, B., Sweet, J., Evans, A., Trachtenberg, J., and Squire, J. (2003). Evidence of multifocality of telomere erosion in high-grade prostatic intraepithelial neoplasia (HPIN) and concurrent carcinoma. Oncogene *22*, 1978–1987.

Wang, S., Gao, J., Lei, Q., Rozengurt, N., Pritchard, C., Jiao, J., Thomas, G.V., Li, G., Roy-Burman, P., Nelson, P.S., et al. (2003). Prostate-specific deletion of the murine Pten tumor suppressor gene leads to metastatic prostate cancer. Cancer Cell *4*, 209–221.

Weinstein, I.B. (2002). Cancer. Addiction to oncogenes—The Achilles heal of cancer. Science *297*, 63–64.

Wong, S., McLaughlin, J., Cheng, D., Zhang, C., Shokat, K.M., and Witte, O.N. (2004). Sole BCR-ABL inhibition is insufficient to eliminate all myeloproliferative disorder cell populations. Proc. Natl. Acad. Sci. USA *101*, 17456–17461.

Xin, L., Ide, H., Kim, Y., Dubey, P., and Witte, O.N. (2003). In vivo regeneration of murine prostate from dissociated cell populations of postnatal epithelia and urogenital sinus mesenchyme. Proc. Natl. Acad. Sci. USA *100* (*Suppl 1*), 11896–11903.

Xin, L., Teitell, M.A., Lawson, D.A., Kwon, A., Mellinghoff, I.K., and Witte, O.N. (2006). Progression of prostate cancer by synergy of AKT with genotropic and nongenotropic actions of the androgen receptor. Proc. Natl. Acad. Sci. USA *103*, 7789–7794.

Zambrano, A., Kalantari, M., Simoneau, A., Jensen, J.L., and Villarreal, L.P. (2002). Detection of human polyomaviruses and papillomaviruses in prostatic tissue reveals the prostate as a habitat for multiple viral infections. Prostate *53*, 263–276.

Zhang, X., Ibrahimi, O.A., Olsen, S.K., Umemori, H., Mohammadi, M., and Ornitz, D.M. (2006). Receptor specificity of the fibroblast growth factor family. The complete mammalian FGF family. J. Biol. Chem. *281*, 15694–15700.

Zhong, C., Saribekyan, G., Liao, C.P., Cohen, M.B., and Roy-Burman, P. (2006). Cooperation between FGF8b overexpression and PTEN deficiency in prostate tumorigenesis. Cancer Res. *66*, 2188–2194.